PRAMANA — journal of physics

Vol. 82, No. 1
January 2014
pp. 29–38

Development of coherent tunable source in 2–16 μm region using nonlinear frequency mixing processes

UDIT CHATTERJEE
Laser Laboratory, Physics Department, Burdwan University, Burdwan 713 104, India
E-mail: duitudit@yahoo.com

DOI: 10.1007/s12043-013-0640-2; ***e*Publication:** 9 January 2014

Abstract. A very convenient way to obtain widely tunable source of coherent radiation in the infrared region is through nonlinear frequency mixing processes like second harmonic generation (SHG), difference-frequency mixing (DFM) or optical parametric oscillation (OPO). Using commonly available Nd:YAG laser and its harmonic pumped dye laser radiation as parent beams, we have been able to generate coherent tunable infrared radiation (IR) in 2–16 μm region using different nonlinear crystals by DFM and OPO. We have also generated such IR source in the 4–5 μm region through SHG of CO_2 laser in different infrared crystals. In the process we have characterized a large number of nonlinear crystals like different borate group of crystals, KTP, KTA, $LiIO_3$, MgO:$LiNbO_3$, GaSe, $AgGaSe_2$, $ZnGeP_2$, $AgGa_{1-x}In_xSe_2$, $HgGa_2S_4$ etc. To improve the conversion efficiencies of such frequency conversion processes, we have developed some novel schemes, like multipass configuration (MC) and positive optical feedback (POF). The significance of the obtained results lies in the fact that to get the same conversion in SHG or DFM, one now requires fundamental input radiation with much lower intensity.

Keywords. Nonlinear frequency conversion; infrared radiation; nonlinear materials

PACS Nos 42.65.Ky; 42.70.Mp; 42.70.Km; 07.57.Hm

1. Introduction

Coherent tunable infrared radiation (IR) in the 2–16 μm range has many important applications in high resolution spectroscopy, remote sensing, trace gas and vapour detection, material diagnostics, military applications such as target tracking, IR countermeasures and also in laser isotope separation. The region includes both the atmospheric windows, namely, 3–5 μm and 8–12 μm. The first window region, the so-called 'molecular fingerprint' region [1] of the spectrum can be effectively exploited for detecting atmospheric trace gases like CH_4 (3.39 μm), H_2CO (3.49 μm), HCl (3.52 μm), HBr (3.78 μm), N_2O (4.53 μm), CO (4.67 μm), OCS (4.87 μm) etc. (major absorption peak shown in bracket). The 8–12 μm region contains such characteristic absorption peaks for CF_4, NH_3, O_3, CO,

glucose etc. A proposed important application of mid-infrared sources had been non-invasive medical diagnostics, e.g. the glucose or blood sugar level in a diabetic patient can be monitored non-invasively by passing IR light through the person's ear lobe and measuring the attenuation at the glucose resonances near 9 μm thereby enabling continuous monitoring of glucose levels without taking blood samples [2]. Finally, IR radiation at 16 μm can be very effectively used for uranium enrichment.

The nonlinear frequency conversion processes (NFCP) such as difference frequency mixing (DFM), optical parametric oscillation (OPO) and also second harmonic generation (SHG) utilizing different fundamental laser sources and suitable nonlinear crystals offer broadly tunable coherent radiation in the IR region. Using commonly available Nd:YAG laser and its harmonic pumped dye laser radiation as parent beams, we have been able to generate coherent tunable infrared radiation in 2–16 μm region using different nonlinear crystals by DFM. We have also generated such source in the 4–5 μm region through SHG of CO_2 laser in different infrared crystals. In the process we have characterized a large number of nonlinear crystals that include borate group of crystals, KTA, $LiIO_3$, MgO:$LiNbO_3$, GaSe, $AgGaSe_2$, $ZnGeP_2$, $AgGa_{1-x}In_xSe_2$ and $HgGa_2S_4$. We have developed some novel schemes, like multipass configuration (MPC) and positive optical feedback (POF) for the substantial enhancement of the conversion efficiencies. The significance of the obtained results is that, to get the same conversion in SHG or DFM, one now requires fundamental input radiation with much less intensity.

In the heart of the NFCP lays the nonlinear crystal. For efficient IR generation it is quite advantageous if the crystal allows the use of 1 μm radiation (Nd:YAG and Yb:fibre) as one of the pump beams. Apart from that, the desirable properties of such a crystal include (i) high nonlinear coefficient, (ii) wide IR transparency and adequate birefringence, (iii) low absorption loss at the interacting radiations, (iv) high laser damage threshold, (v) low thermal lensing, i.e., should have high thermal conductivity and low thermo-optic coefficient dn/dT, (vi) good mechanical and environmental (not hygroscopic) stability and (vii) the ability to grow to large size with good optical uniformity. The present article reviews the important characterization works done at our facility as well as some recent significant developments on such IR generating crystals.

2. Borate group of crystals

A number of borate group crystals, such as BBO, CLBO, LB_4 etc. had been used for generating near-infrared radiation (NIR) in the 2–3 μm range. Our laboratory was the first to demonstrate the generation of tunable NIR (2.04–3.42 μm) by Type-I DFM in BBO using second harmonic of Nd:YAG laser and tunable dye laser as fundamental beams [3]. Several researchers [4,5] demonstrated efficient OPO in this crystal to generate NIR using third harmonic of the Nd:YAG laser radiation. In another notable work, a large tunability from 0.354 to 2.37 μm was obtained in a 12 mm long Type-I, $\theta = 32^\circ$ cut BBO crystal using 308 nm as pump beam from an Excimer laser. Three sets of mirrors having high transmission at 308 nm and with high reflectance ($\sim$90–95%) over the signal wavelength ranges (320–370, 420–480 and 500–600 nm) were used to cover this tuning range [6]. CLBO is another borate crystal that can be used for NIR generation. It can be grown to large size with good optical quality within a very short time frame and

its laser damage threshold is two times larger than BBO [7]. We have demonstrated [8] tunable (2.2–2.74 μm) NIR generation in it using our existing Nd:YAG and dye system and have shown that this highly hygroscopic crystal works well only at humidity levels below 45% [9]. The nonhygroscopic negative uniaxial borate crystal LB_4 (lithium tetraborate) has the highest laser damage threshold among all nonlinear crystals till to date and it transmits till 3.5 μm [10]. It can easily be grown to large size with very good optical and mechanical quality. Although we have demonstrated the generation of NIR till 2.3 μm in this crystal [11], and generation up to 3.5 μm is also phase matchable using Nd:YAG and dye laser radiation, but the crystal offers very low effective nonlinear coefficient. Other borate crystals, namely, KBBF, SBBO, TBO, BABO etc. had been reported to have transmission till 3.5 μm [12]. Their NIR generation potentials are yet to be evaluated.

3. KTA, MgO:$LiNbO_3$ and $LiIO_3$

The positive biaxial crystal KTA, an analog of KTP, has several advantages over KTP. Good quality crystals of KTA in large size had been developed that are free from grey-track as well as multidomain effects. Its transmission cut-off is ∼5.3 μm which is about 1 μm longer than KTP. Moreover, phosphate group overtones absorption between 3 and 4 μm which is a characteristic of KTP is absent in this crystal. Generation up to 5.2 μm as against ∼4 μm in KTP had been confirmed in this crystal [13,14]. By DFM of 1.064 μm from an injection-seeded Nd:YAG laser (220 mJ energy) and 750–920 nm tunable radiation from a single mode Ti:sapphire laser (80 mJ energy throughout the entire tuning range) in a x–z cut ($\theta = 40°, \phi = 0°$), 8 mm long KTA crystal, Kung [13] had reported the generation of continuously tunable IR radiation from 2.65 to 5.25 μm with ∼15 mJ output in 2.66–3.5 μm, ∼5 mJ output in 4–4.5 μm and much less than 1 mJ output in regions longer than 5 μm. Superiority of parametric mixing in x–z direction in KTA owing to its 2.45 times higher effective nonlinearity compared to y–z direction was also confirmed. In a Type-II, $\theta = 41°$ and $\phi = 0°$ cut, 15 mm long KTA crystal utilizing DFM of second harmonic (λ_1) of Nd:YAG laser and the same pumped tunable dye laser radiation (λ_2, 562–650 nm) we were able to obtain as high as 6 mJ energy in 3–3.5 μm (λ_3) region while <1 mJ energy in 4–5 μm region. Figure 1 shows the experimental diagram. A maximum conversion efficiency $\eta \left[= 100 \times I_3/(I_1 I_2)^{1/2}\ \%\right]$ of 8.6% was achieved for the generation of 3 μm when both the input beams have 70 mJ of energy. This corresponds to a quantum conversion efficiency ($I_3\lambda_3/I_1\lambda_1$) of ∼67%. With the DFM output we scanned both the fundamental (ν_3) and the first overtone ($2\nu_3$) bands of methane at 90 Torr pressure in a laboratory-made single pass gas cell of 33 cm length [15]. We did not use any linewidth narrowing element like etalon in the input dye beam cavity. But still the obtained spectral resolution of the generated IR was seen to be <1 cm^{-1} (FWHM) as obtained by fitting the Lorentzian line profile for the measured spectrum of P(5) line of ν_3 band of methane.

Obviously, the presence of 90° rotator and whether the SHG DKDP crystal be rotated in vertical plane, i.e. in effect what should be the polarizations of the input beams, will be determined by the nonlinear crystal chosen to generate IR. In figure 1, since the set-up is shown for KTA, the DKDP crystal was rotated in vertical plane so

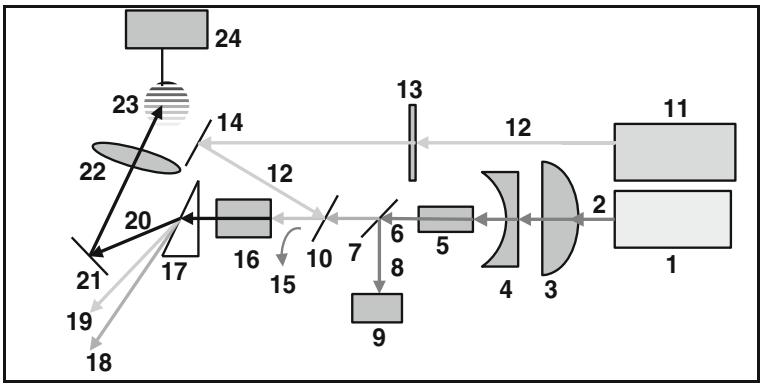

Figure 1. Schematic of the general set-up for collinear DFM for the generation of IR radiation. **1**: Nd:YAG laser; **2**: 1064 nm beam; **3** and **4**: Lenses for telescopic focussing arrangement; **5**: DKDP crystal for SHG; **6**: 532 nm beam used for DFM in KTA; **7**: Dichoric mirror with high R (∼99.8%) for 1064 nm and high T (>99%) for 532 nm; **8**: Residual 1064 nm beam; **9**: Beam dump for 1064 nm radiation; **10**: Dichoric mirror having high R (∼99.5%, broadband coating) for dye beam and high T (>99%) for 532 nm; **11**: Dye laser **12**: Tunable dye beam; **13**: 90° rotator for dye radiation; **14**: Mirror with high R (∼99.8%) for dye radiation (broadband coating); **15**: Combined dye and 532 nm beams; **16**: KTA for DFM; **17**: MgF_2 prism; **18**: Residual 532 nm beam; **19**: Residual dye beam; **20**: Generated tunable IR radiation; **21**: Aluminum-coated mirror for IR radiation; **22**: CaF_2 lens; **23**: Sensor head of power/energy meter; **24**: Power/energy meter read-out unit.

that the generated SHG (532 nm) beam became vertically polarized while the presence of 13 made the dye radiation horizontally polarized. Line tunable singly resonant OPO in 3–5 μm region had been demonstrated in this crystal as well using Nd:YAG laser radiation as pump [16,17]. In our lab, the maximum energy at 3.6 μm radiation with a grating having 85 l/mm grooves density at 55 mm cavity length was 4.6 mJ when the cavity was pumped by 42.6 mJ energy. This corresponds to 10.8% conversion from pump beam energy to the generated idler beam energy and maximum slope efficiency achieved was 23.6% [16]. The linewidth obtained with a grating having 600 l/mm grooves density at 3.7 μm was 0.53 cm^{-1}.

The negative uniaxial crystal $LiNbO_3$ had attracted attention from the early days of nonlinear frequency conversion experiments. Due to its large nonlinearity, capability of noncritical phase-matching, the fact that large-sized crystal of good optical quality can be grown and also for its large transmission range (0.33–5.5 μm), the crystal had been used extensively in a wide variety of NFCP. However, the crystal suffers from large photorefractive effect owing to which its laser damage threshold is quite low. Around 1980, it was suggested [18] that doping (usually 5 mole%) of $LiNbO_3$ by magnesium oxide (MgO) considerably reduces photorefractive damage. Till then, doping with ZnO, In_2O_3 etc. had also been reported [19]. As high as 23% conversion efficiency to the idler wavelength around 3.5 μm was obtained in a nanosecond (∼3.6 ns) OPO using 1.064 μm

from single longitudinal mode Nd:YAG laser as pump. The OPO consisted of a 12 × 12 × 50 mm^3 $LiNbO_3$ crystal cut at $\theta = 48°$ and $\phi = 90°$. The pump beam diameter was 8 mm. A maximum energy of 105 mJ at 3.5 μm was obtained for 450 mJ pump [20]. Tuning range obtained was from 2.85 μm to 4.2 μm. Efficiency however was reduced to 15% in 4 μm region from maximum efficiency at 3.5 μm. Using Nd:YAG laser radiation as the pump, we started preliminary OPO experiment with a 30 mm long MgO:$LiNbO_3$ crystal Type-I cut at $\theta = 44°$, $\phi = 90°$ that had been procured from Casix Inc, China. We had obtained tunable output in 2–3.5 μm region and observed that our experimental data of phase-matching angle follow closely with those predicted using Sellmeier relations of Zelmon *et al* [21]. However, an interesting but somewhat complicated temperature-dependent Sellmeier relation had also been reported [22] which is also worth trying for predicting the phase-matching angle in the IR region. Further work is going on in our laboratory to extend the tunability range up to 4 μm.

The negative uniaxial $LiIO_3$ is another important nonlinear crystal offering good transmission in the 3–5 μm region. Starting from 0.3 μm in UV, its transmission extends till ∼6.0 μm in IR. This large transmission in one single crystal, its large nonlinearity and that it can be grown to large size (∼50 mm length) with very good optical quality, compensate some of its important drawbacks like highly hygroscopic nature, quite low laser damage threshold and large walk-off effect. One usually has to use critical phase-matching with unfocussed beam of considerable size to avoid walk-off. This also allows the use of greater crystal volume and also higher input energy to get higher efficiency without damaging the crystal. We have done DFM of 532 nm and the same pumped tunable dye laser radiation in a 30 mm long Type-I $\theta = 22°$ cut $LiIO_3$ crystal. We have employed tangential phase-matching (TPM) configuration by which we have realized an internal angular tolerance as large as ∼4.6 mrad over the pump beam (532 nm). This is an order of magnitude higher than the obtained value for any other phase-matching configuration [23]. Moreover, TPM being a noncollinear configuration, the generated beam got automatically separated from its parent input beams without any need of beam separating filters. This enabled us to obtain a conversion efficiency of 1.8% at 3.8 μm from pump to IR with pump beam intensity of only 25 MW/cm^2 (the dye beam intensity being 71 MW/cm^2). Even considering the walk-off limitation of our system, the obtained conversion was double that of the earlier reported values with 50 mm long sample with slightly higher pump beam intensity. We have further found out a transmission window region between 6.6 and 7.9 μm beyond the two-photon cut-off limit of 6 μm in this crystal and demonstrated the plausibility of generating 6.8–7.7 μm with sufficient intensity to study absorption spectra of different samples in our laboratory [24].

4. IR Crystals

$ZnGeP_2$, $AgGaSe_2$, $AgGaS_2$ and $CdGeAs_2$ crystals are well-studied and important nonlinear IR transmitting crystals. A number of reports had been made on SHG of tunable CO_2 laser radiation to generate IR radiation in 4–5 μm region. All these crystals had very low laser damage threshold which prevent the use of high input fundamental power density to enhance conversion efficiency. Moreover, $ZnGeP_2$ has high radiation loss of

fundamental modes of CO_2 laser radiation, and the prospect of making OPO or DFM faces the problem that the short wavelength cut-off in this crystal limits the choice of pump lasers to those operating at wavelengths >2 μm. Present research gives special attention to reduce the defect-related absorption loss to ~2 μm in this crystal. Using 2.08 μm as pump a number of reports have been made for OPO and/or OPA in $ZnGeP_2$ for generating IR radiation in 3–5 μm with energy greater than 25 mJ [25–27]. We have explored the possibility of the temperature-dependent phase-matched SHG of tunable CO_2 laser radiation [28] to generate 4.6–4.8 μm in this positive uniaxial crystal having high nonlinear figure of merit $\left(d_{\text{eff}}^2/n^3\right)$. Recently, high-power SHG of pulsed TEA CO_2 laser at 9.3 μm had been reported [29] wherein an average power of 20.3 W was obtained at 250 Hz using a parallel array of seven 12 mm-long $ZnGeP_2$ crystals with a fundamental energy density of 1.0 J/cm^2. The authors have done the same experiment with $AgGaSe_2$ and reported the damage threshold of $ZnGeP_2$ to be ~4 times higher than that of $AgGaSe_2$. In the negative uniaxial crystal $AgGaSe_2$, SHG can be realized in the range $3.0 < \lambda < 16.0$ μm although it has transmission till 17.0 μm. Type-I SHG of CO_2 laser radiation with 14% conversion efficiency is reported in [30]. We studied change of refractive indices and absorption characteristic with temperature and determined the thermo-optic coefficient (dn/dT) for this crystal and confirmed its poor thermal properties [31]. A novel technique of controlling crystal birefringence by varying the crystal composition had been used to obtain new IR-mixed crystals that had larger transparency ranges and higher nonlinearities compared to parent crystals. We first demonstrated 10% higher efficiency for SHG of CO_2 laser in such a mixed crystal grown by the scheme $AgGaSe_2$(65%):$AgInSe_2$(35%) $\rightarrow$ $AgGa_xIn_{1-x}Se_2$ (where x is the mixing ratio) as compared to its parent crystals [32]. Experimental investigations of the SHG in $AgGa_{0.65}In_{0.35}Se_2$, $AgGaSe_2$ and $ZnGeP_2$ crystals first demonstrated that their efficiencies are in the ratios 10.9:4.1:6.8%, which confirms the superiority of the mixed $AgGa_xIn_{1-x}Se_2$ crystals [33,34]. We have characterized $HgGa_2S_4$,another important negative uniaxial IR crystal for SHG of tunable CO_2 laser radiation. It offers large IR transmission coupled with wide visible transmission (0.5–13 μm) and has better figure-of-merit than $AgGaSe_2$, $ZnGeP_2$ and GaSe. Its laser damage threshold is higher than $AgGaSe_2$. We have confirmed [35] that this crystal is about 1.5 times better than the indium-doped GaSe, about three times better than that of $AgGa_xIn_{1-x}Se_2$ but about 2.5 times less efficient than $ZnGeP_2$. To obtain tunable IR radiation from 5 to 16 μm, we have used indium-doped GaSe crystal. The negative uniaxial crystal GaSe is a layered-structure crystal that has a high nonlinear coefficient ($d_{22} = 54$ pm/V) and a wide visible-to-IR transmission (0.65–18.0 μm) and thus is suitable for pumping with a Nd:YAG laser at 1.064 μm. Its nonlinear figure-of-merit is about four times higher than that of $AgGaSe_2$ but slightly less than that of $ZnGeP_2$. Its soft layered structure makes it difficult to cut, polish and coat although it has now been demonstrated that doping with indium improves its structural properties allowing crystals to be cut at arbitrary angles without significantly altering its optical and nonlinear properties [36]. We have used DFG–DFG technique using a 0° cut, 10-mm thick GaSe crystal with doping concentration of indium to be 0.5% by mass. In the first stage, 1.135–1.35 μm was generated by DFG of Nd:YAG and tunable dye laser radiation in a BBO crystal. In the next stage, this NIR was used with Nd:YAG laser radiation for DFM in indium-doped GaSe to obtain tunable IR radiation in 5–16 μm region [37]. Some good reviews on these and many other IR crystals are given in [38,39].

5. Novel techniques to improve conversion efficiency

Conversion efficiency (η) of frequency mixing processes is directly proportional to the square of the length (L) of the crystal. However, the effective length (L_{eff}) can be much less than L if the crystal has large walk-off effect as in the case of BBO, $LiIO_3$ etc. The first method we have developed, as shown in figure 2, is the MPC for SHG in two identical crystals with their optic axes rotated by 90°. Thus, if the fundamental laser radiation makes m number (m is even) of passes through the crystal of length L, besides the effective crystal length being mL, walk-off effect in one crystal gets compensated in the next one. Thus η increases by m^2 times compared to the single pass [40].

We demonstrated an improvement of η by SHG of Nd:YAG laser radiation utilizing this scheme in LB_4. We also made theoretical calculation [41] for SHG of CO_2 laser radiation in $AgGaSe_2$ (table 1). Obviously, this direct L^2 relation is valid for $\eta < 10\%$. For higher single-pass conversion, of course one has to take into account the pump depletion effect. For example, in a 20 mm long $AgGaSe_2$ with 4 pass, one gets $L_{\text{eff}} = 80$ mm and hence compared to single-pass SHG, there should be 16 times improvement in η. But the pump depletion effect reduces it to 5 times. However, this still indicates considerable improvement over single pass.

The second novel scheme that we have successfully demonstrated is the POF configuration where the residual energy of one of the input parent beams after conventional first-pass generation is fed back into the original set-up thereby increasing its energy for further conversion. However, the scheme will be applicable for those interactions where one of the input fundamental radiations itself is a secondary coherent source and not a primary laser, i.e. radiations coming out of an oscillator configuration must not be coherent, e.g., output from different standard lasers including dye laser as well as that from OPO. The coherent radiations obtained by extra-cavity NFCP including SHG of such primary sources in suitable nonlinear media are designated here as secondary coherent sources. Figure 3 shows our proposed set-up for DFM in $LiIO_3$ using POF. For theoretical calculation, Type-I, $\theta = 23°$ cut and 20 mm thick crystal is chosen. Then if energies E_2 and

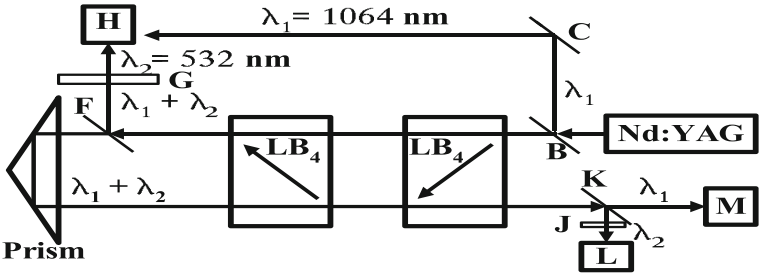

Figure 2. Schematic of the experimental set-up for multipass SHG in twin crystals. **B** is a glass slide used to monitor the fundamental beam energy; **C** is a dichoric mirror for 1064 nm; **F** and **K** are the dichoric mirrors with HT at 1064 nm and HR at 532 nm; **G** and **J** are the filters to block 1064 nm; **M** is the beam dumper for 1064 nm; **H** and **L** are the sensor heads of power/energy meter. For four-pass configuration, mirror **F** must be taken out from the beam path.

Table 1. Intensities of interacting radiations for SHG by MPC.

Fundamental laser radiation	Input intensity (I_F) (MW/cm^2)	Nonlinear crystal	Crystals' configuration	SHG Intensity $(I_{SHG}^{XP})^a$ (MW/cm^2)		Conversion efficiency (%) $(\eta = I_{SHG}^{XP}/I_F)^a$	
				Theor.	Expt.	Theor.	Expt.
1.064 μm (Nd:YAG)	378.2	$Li_2B_4O_7$ ($L = 2$ cm)	F (1 pass)	11.0	10.2	2.9	2.7
			F and G (2 pass)	36.2	31.6	9.6	8.4
			F and G (4 pass)	51.5	43.7	13.6	11.6
	655.7		F (1 pass)	33.0	30.5	5.0	4.7
			F and G (2 pass)	108.9	96.8	16.6	14.8
			F and G (4 pass)	154.6	137.8	23.6	21.0
10.25 μm (CO_2)	5.7	$AgGaSe_2$ ($L = 2$ cm)	F (1 pass)	0.99	–	17.5	–
			F and G (2 pass)	3.78	–	66.83	–
			F and G (4 pass)	4.25	–	91.89	–

[a] X =1, 2 and 4 respectively for 1 pass, 2 pass and 4 pass.

E_d of λ_2 and λ_D are both 45 mJ with 3 mm beam diameter (intensity of 32 MW/cm^2), then by single-pass DFM with Gaussian beams, $LiIO_3$ will generate $E_{IR} \sim 8.6$ mJ at 3.15 μm considering $d_{eff} = 2.2$ pm/V. However, with POF (figure 3), E_{IR} value will increase to 18.8 mJ with the same input energies [42] showing the possibility of marked enhancement.

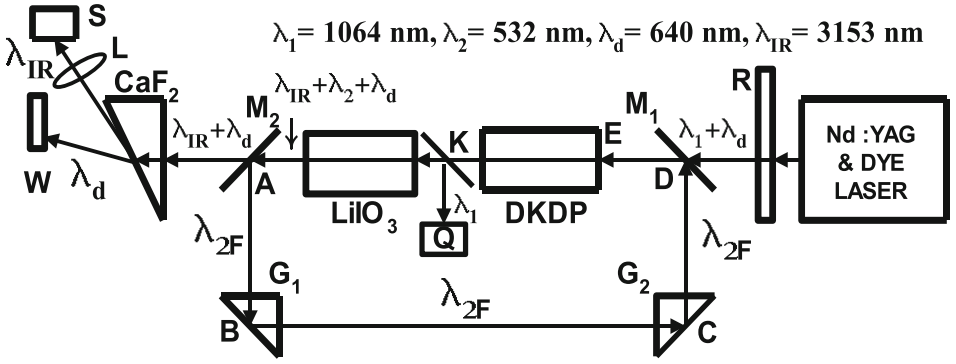

Figure 3. Schematic set-up of DFM employing positive optical feedback for λ_2. **R** is a 90° rotator for dye radiation λ_D; $\mathbf{M}_1$ is the dichoric mirror having HT at λ_1 and λ_D but HR at λ_2; **K** is the dichoric mirror having HT at λ_2 and λ_D but HR at λ_1; **Q** is the beam dumper for λ_1; $\mathbf{M}_2$ is the dichoric mirror having HT at λ_D and generated infrared radiation λ_{IR} but HR at λ_2; $\mathbf{G}_1$ and $\mathbf{G}_2$ are 90° prisms; **ABCD** is the feedback path for residual energy of secondary source λ_2 depicted as λ_{2F} in the return path; CaF_2 prism separates λ_{IR} from λ_D; **L** is a CaF_2 lens and **S** is the IR detector. Polarization rotator like **R** can be introduced in the beam path as per requirement of phase-matching.

6. Conclusion

In conclusion, we have demonstrated that using commonly available Nd:YAG and the same pumped tunable dye laser sources, it is possible to cover a large IR tuning range of 2–16 μm by judicious choice of crystals and phase-matching configurations. A number of new IR crystals having transmission till 13 μm (or greater) like $LiInS_2$, $LiInSe_2$, $AgGaGeS_4$, $Hg_{0.65}Cd_{0.35}Ga_2S_4$ etc. with much better transmission in the visible range had been developed [38] which allows Nd:YAG laser radiation at 1.064 μm to be used as pump. For example, transmission of $LiInS_2$ starts from 340 nm while that of $Hg_{0.65}Cd_{0.35}Ga_2S_4$ starts from 460 nm. Further improvement in the mechanical quality of GaSe by doping to facilitate its cutting and polishing to reduce huge surface reflection loss will be needed as this crystal can give the largest tunability [43]. New novel schemes, like MPC, POF which were developed at our facility, for improving the conversion efficiency of different NFCP have also been discussed.

Acknowledgements

The author acknowledges CAS programme of UGC, Govt. of India for partial financial support for the work.

References

[1] T Topfer, K P Petrov, Y Mine, D Jundt, R F Curl and F K Tittle, *Appl. Opt.* **36**, 8042 (1997)
[2] H C Chui, *Mid-infrared light generation by nonlinear optical frequency conversion in intersubband InGaAs/AlGaAs quantum wells*, Ph.D. Thesis (Dept. of Electrical Engg., Stanford University, 1994) p. 14
[3] G C Bhar, U Chatterjee and S Das, *Appl. Phys. Lett.* **58**, 231 (1991)
[4] Y X Fan, R C Eckardt, R L Byer, J Nolting and R Wallenstein, *Appl. Phys. Lett.* **53**, 2014 (1988)
[5] W R Bosenberg, W S Pelouch and C L Tang, *Appl. Phys. Lett.* **55**, 1952 (1989)
[6] M Ebrahimzadeh, A J Henderson and M H Dunn, *IEEE J. Quant. Electron.* **QE-26**, 1241 (1990)
[7] Y Mori, I Kuroda, S Nakajima, T Ssasaki and S Nakai, *Appl. Phys. Lett.* **67**, 1818 (1995)
[8] U Chatterjee, P Kumbhakar, A K Chaudhary and G C Bhar, *Opt. Commun.* **188**, 371 (2001)
[9] G C Bhar, A M Rudra, P Kumbhakar and U Chatterjee, *Nonlin. Opt.* **23**, 83 (1999)
[10] T Sugawara, R Komatsu and S Uda, *Solid State Commun.* **107**, 233 (1998)
[11] U Chatterjee, P Kumbhakar, A K Chaudhary and G C Bhar, *Appl. Phys. B* **72**, 407 (2001)
[12] C T Chen, L Bai, Z Z Wang and R K Li, *J. Crystal Growth* **292**, 169 (2006)
[13] A H Kung, *Opt. Lett.* **20**, 1107 (1995)
[14] G C Bhar, P Kumbhakar, U Chatterjee and S Das, *Jpn. J. Appl. Phys.* **38**, 2760 (1999)
[15] G C Bhar, P Kumbhakar, A K Chaudhary and U Chatterjee, *Pramana – Phys.* **53**, 321 (1999)
[16] S Das, *IEEE J. Quantum Electron.* **QE-45**, 1100 (2009)
[17] K Zhong, J Q Yao, D G Xu, J I Wang and J S Li, *Appl. Phys. B* **100**, 749 (2010)
[18] G G Zhong, J Jian and Z K Wu, *Proceedings of 11th Int. Quantum Electron. Conf.* (1980) p. 631
[19] D Xue and K Betzler, *Appl. Phys. B* **72**, 641 (2001)
[20] J Avidor, ISORAD, Electrooptics Division, Israel (1995) private communication
[21] D E Zelmon, D L Small and D Jundt, *J. Opt. Soc. Am. B* **14**, 3319 (1997)

[22] J Q Yao, Y Z Yu, W Lu, P Wang, Z Y Wang, H J Peng and H S Kwok, *Adv. Solid State Lasers Conf., Technical Digest* (2001) p. 279
[23] U Chatterjee, A M Rudra and G C Bhar, *Opt. Commun.* **118**, 367 (1995)
[24] U Chatterjee, A M Rudra and G C Bhar, *Appl. Phys.* **61**, 489 (1995)
[25] G Rustad, S Nicolas, Ø Nordseth and G Arisholm, *Proc. SPIE* **5989**, Article No. 598904 (2005)
[26] A Dergachev, D Armstrong, A Smith, T Drake and M Dubois, *Proc. SPIE* **6875**, Article No. 687507 (2008)
[27] M W Haakestad, G Arisholm, E Lippert, S Nicolas, G Rustad and K Stenersen, *Proc. SPIE* **7115**, Article No. 71150Q (2008)
[28] G C Bhar, S Das and U Chatterjee, *Appl. Phys. Lett.* **89**, 313 (1989)
[29] D J Li, J Guo, G L Yang, F J Meng, L M Zhang, J J Xie, F Chen, C L Shao, C S Zhang, Y M Zeng and S M Li, *Laser Phys.* **22**, 725 (2012)
[30] R C Eckardt, Y X Fan, R K Route, R S Feigelson and J Van der Laan, *Appl. Phys. Lett.* **47**, 786 (1985)
[31] G C Bhar, S Das, U Chatterjee, A M Rudra, R K Route and R S Feigelson, *J. Appl. Phys.* **74**, 5282 (1993)
[32] G C Bhar, S Das, U Chatterjee, P K Datta and Yu N Andreev, *Appl. Phys. Lett.* **63**, 1316 (1993)
[33] G C Bhar, S Das, D V Satyanaryan, P K Datta, U Nundy and Yu N Andreev, *Opt. Lett.* **20**, 2057 (1995)
[34] Yu N Andreev, I V Baturin, P P Geiko and A I Gusamov, *Kvant. Elektron.* **29**, 66 (1999)
[35] S Das, U Chatterjee, C Ghosh, S Gangopadhyay, Yu M Andreev, G Lanskii and V V Badikov, *Opt. Commun.* **259**, 868 (2006)
[36] D R Suhre, N B Singh, V Balakrishna, N C Fernelius and F K Hopkins, *Opt. Lett.* **22**, 775 (1997)
[37] S Das, C Ghosh, S Gangopadhyay, U Chatterjee and Yu M Andreev, *J. Opt. Soc. Am. B* **23**, 282 (2006)
[38] M V Kabanov, Yu M Andreev, V V Badikov and P P Geiko, *Russian Phys. J.* **46**, 835 (2003)
[39] P D Mason and L F Michaille, *Proc. SPIE* **7115**, Article No. 71150N (2008)
[40] U Chatterjee, S Gangopadhyay, C Ghosh and G C Bhar, *Appl. Opt.* **44**, 817 (2005)
[41] U Chatterjee, C Ghosh, S Gangopadhyay and S Das, *Proc. ICOL-2005*, Article No. OP-NLO-7, Dehradun (2005)
[42] U Chatterjee and S Gangopadhyay, *Proc. MMSETLSA* (Allahabad, 2009) p. 3
[43] W Shi and Y J Ding, *Appl. Phys. Lett.* **84**, 1635 (2004)